Regimes of stratified turbulence at low Prandtl number

K. Shah, G. P. Chini, C. P. Caulfield, and P. Garaud

(Received xx; revised xx; accepted xx)

Quantifying transport by strongly stratified turbulence in low Prandtl number (Pr) fluids is critically important for the development of better models for the structure and evolution of stellar and planetary interiors. Motivated by recent numerical simulations showing strongly anisotropic flows suggestive of scale-separated dynamics, we perform a multiscale asymptotic analysis of the governing equations. Our analysis reveals the existence of several distinct dynamical regimes depending on the emergent buoyancy Reynolds and Péclet numbers, $Re_b = \alpha^2 Re$ and $Pe_b = Pr Re_b$, respectively, where α is the aspect ratio of the large-scale turbulent flow structures, and Re is the outer scale Reynolds number. Scaling relationships between the aspect ratio and the strength of the stratification, measured by the Froude number Fr, naturally emerge from the analysis. When $Pe_b \ll \alpha$, our results recover the scaling laws empirically obtained from direct numerical simulations of Cope *et al.* (2020). For $Pe_b \geqslant O(1)$, we find that $\alpha \sim Fr$. This scaling is consistent with the results of Chini *et al.* (2022) on strongly stratified geophysical turbulence at $Pr = O(1)$. Finally, we have identified a new regime for $\alpha \ll Pe_b \ll 1$, in which slow, large scales are diffusive while fast, small scales are not. We conclude by presenting a map of parameter space that clearly indicates the transitions between isotropic turbulence, non-diffusive stratified turbulence, diffusive stratified turbulence and viscously-dominated flows.

Key words:

1. Introduction

PG: have not touched this yet. KS: Intro needs a complete rewrite, let's do it at the end. GPC: I did some light editing nevertheless. Shear-driven turbulence in the stratified regions of planetary oceans, atmospheres, stellar interiors, and gas giants provides an important source of vertical transport of heat, momentum, and chemical tracers. Spiegel & Zahn (1970) and Zahn (1974) realized, however, that stratified turbulence in stars and planets differs fundamentally from geophysical turbulence because the Prandtl number Pr, the ratio of the kinematic viscosity ν to the thermal diffusivity κ_T, is very small. Indeed, in stably stratified geophysical systems such as Earth's atmosphere and oceans, typically $Pr = 0.7$ and $Pr = 10$, respectively. When $Pr = O(1)$, turbulent flows (with outer-scale Reynolds numbers $Re \gg 1$) are always thermally non-diffusive. This conclusion follows because the ratio of the thermal diffusion time scale to the turbulent advection time scale, the Péclet number Pe, satisfies $Pe = Pr Re$, implying that when $Pr = O(1)$, $Pe = O(Re)$. In stellar radiation zones of solar-type and intermediate-mass stars, Pr ranges from 10^{-9} to 10^{-5} (Garaud 2021). With $Pr \ll 1$ and $Pe \ll Re$, it is possible to have $Pe \ll 1 \ll Re$, i.e. regimes of thermally diffusive stratified turbulence, which is not possible in geophysical fluids.

Stratified turbulence in stars is thought to be generated by horizontal shear instabilities (Zahn 1992). In a horizontal shear flow, due to the high stratification and low viscosity, the turbulent eddies are flat and only weakly coupled in the vertical direction. Their characteristic vertical scale H is far smaller than their characteristic horizontal scale L, such that the aspect ratio $\alpha = H/L \ll 1$. Relative horizontal motion between the eddies then produces vertical shear on the vertical length scale which can in some circumstances become unstable and generate vertical mixing. As turbulence in stars is difficult to observe, numerical simulations of strongly stratified, $Pr \ll 1$ flows yield considerable insight into the validity of the Zahn (1992) mechanism. Numerical simulations at low (Cope *et al.* 2020) and high (Garaud 2020) Pe exhibit layerwise horizontal motions, supporting Zahn's horizontal shear instability mechanism for stratified stellar turbulence. The flows are strongly anisotropic and exhibit scale separation, as predicted.

Scaling relationships have been proposed to characterise the interplay between the flow anisotropy, measured by α, the characteristic vertical velocity of the turbulent eddies w_{rms}, and the stratification, measured by the inverse Froude number Fr^{-1}, the ratio of the buoyancy frequency N to the horizontal shearing rate U/L of the large-scale flow; i.e. scaling relationships between

$$\alpha = \frac{H}{L} \quad \text{and} \quad Fr = \frac{U}{NL}. \tag{1.1}$$

In geophysical flows that necessarily have large Pe (and $Pr = O(1)$), Billant & Chomaz (2001) proposed that $\alpha, w_{rms} \propto Fr$. Chini *et al.* (2022) more recently argued using multiscale analysis that $\alpha \propto Fr$ but $w_{rms} \propto Fr^{1/2}$ in the same regime. At large Pe (but low Pr), Garaud (2020) tentatively proposed that $\alpha, w_{rms} \propto Fr^{2/3}$ could explain her numerical simulations results. At low Pe, two distinct scalings have been proposed: $\alpha, w_{rms} \propto Fr_M$ from critical balance theory (Skoutnev 2023) and $\alpha \propto Fr_M^{4/3}$, $w_{rms} \propto Fr_M^{2/3}$ from numerical simulations (Cope *et al.* 2020). Here,

$$Fr_M = \left(\frac{U\kappa_T}{N^2 L^3} \right)^{1/4} \tag{1.2}$$

is a modified Froude number, the ratio of the horizontal shearing rate to . . . ??, introduced by Lignières (1999) and Skoutnev (2023) to account for the effect of thermal dissipation.

GPC: Haven't really touched this last paragraph. In this study, we begin by summarizing previous results obtained by a simple rescaling of the governing equation that emphasizes the expected anisotropy of the turbulence on the large scales. Noting, however, that the turbulence in DNS exhibits both large and small scales (add citations), we revisit the problem by conducting a slow-fast decomposition of the governing equations at high Pe_b (§**??**) and low Pe_b (§**??**). We identify a new regime at intermediate values of Pe_b, where the mean flow occurs at low Péclet number but the fluctuation dynamics do not. We extend the multiscale analysis of Chini *et al.* (2022) (briefly summarized in §**??**) to low Pr. When the mean and fluctuations are both low Pe_b, we demonstrate that the Cope *et al.* (2020) scaling relationships between α, w_{rms} and Fr_M naturally emerge (§**??**). Additionally, we derive a multiscale model for the regime at intermediate values of Pe_b. We use this analysis to partition the parameter space into various regimes of stratified turbulence at low Pr (§4.2) and then conclude by discussing possible implications for the expected dynamics of stellar radiation zones in §5.

2. Governing equations and anisotropic scalings

Consider a three-dimensional, non-rotating, incompressible flow expressed in a Cartesian coordinate system where the vertical coordinate z (with unit vector $\hat{\boldsymbol{e}}_z$) is anti-aligned with gravity ($\mathbf{g} = -g\hat{\boldsymbol{e}}_z$). The fluid is stably stratified, and has a mean density ρ_0 and a constant background buoyancy frequency N. Buoyancy perturbations away from this mean state are incorporated in accordance with the Boussinesq approximation (Spiegel & Veronis 1960). A body force $F^*\hat{\boldsymbol{e}}_x$ is applied to drive a mean horizontally sheared flow (where F^* is a function of the spanwise variable y^* only, and $\hat{\boldsymbol{e}}_x$ is the unit vector in the streamwise, i.e. x^*, direction). The dimensional governing equations are

$$\frac{\partial \boldsymbol{u}^*}{\partial t^*} + \boldsymbol{u}^* \cdot \boldsymbol{\nabla}^* \boldsymbol{u}^* = -\frac{1}{\rho_0}\nabla^* p^* + b^*\hat{\boldsymbol{e}}_z + \nu\nabla^{*2}\boldsymbol{u}^* + \frac{F^*(y^*)}{\rho_0}\hat{\boldsymbol{e}}_x, \tag{2.1a}$$

$$\boldsymbol{\nabla}^* \cdot \boldsymbol{u}^* = 0, \tag{2.1b}$$

$$\frac{\partial b^*}{\partial t^*} + \boldsymbol{u}^* \cdot \boldsymbol{\nabla}^* b^* + N^2 w^* = \kappa\nabla^{*2} b^*, \tag{2.1c}$$

where $\boldsymbol{\nabla}^* = (\partial/\partial x^*, \partial/\partial y^*, \partial/\partial z^*)$, $\boldsymbol{u}^* = (u^*, v^*, w^*)$ denotes the velocity field, p^* the pressure, and b^* the buoyancy perturbation with respect to the background stratification. Starred dependent and independent variables are dimensional quantities. In accord with the Boussinesq approximation, the fluid has a constant kinematic viscosity ν and constant diffusivity κ. We omit the stars from the constants describing the fluid properties ρ_0, ν, κ and N for simplicity of notation, but these parameters are dimensional. All perturbations from the stratified rest state are assumed to be triply periodic in a domain of size (L_x^*, L_y^*, L_z^*). Accordingly, the body force is also assumed to be periodic in y^*, with a characteristic length scale $L^* \leqslant L_y^*$.

2.1. *Anisotropic scalings at $Pr = O(1)$*

In the limit of strong stratification, vertical displacements are energetically costly, and fluid motions become strongly anisotropic (with $u^*, v^* \gg w^*$). This anisotropization has been demonstrated in numerical simulations, laboratory experiments, and *in situ* observations XXXX cite lots of papers XXX, and suggests that one should non-dimensionalise the governing equations (2.1) anisotropically. Billant & Chomaz (2001) and Brethouwer *et al.* (2007) have argued that the (dimensional) horizontal and vertical length scales of turbulent eddies ought to be L^* and H^*, respectively, with an aspect ratio

$$\alpha \equiv \frac{H^*}{L^*} \ll 1. \tag{2.2}$$

We thus introduce a new vertical coordinate ζ^* such that

$$z^* = \alpha\zeta^*. \tag{2.3}$$

Consequently, if the horizontal velocity scale is U^*, then the vertical velocity scale must be αU^* to respect the divergence free condition without overly restricting the allowable types of flows. Time should be scaled by the turnover time of the horizontal eddies L^*/U^*, and pressure by $\rho_0 U^{*2}$. To ensure that the nonlinear terms balance the forcing, $U^* = (F_0^* L^*/\rho_0)^{1/2}$, where F_0^* is the characteristic forcing amplitude. Finally, the buoyancy scale is chosen to be $H^* N^2$ to ensure that vertical advection of the the background stratification enters the buoyancy equation at leading order and balances the horizontal advection of the buoyancy fluctuations.

Denoting the horizontal components of the velocity as $\boldsymbol{u}_\perp = (u, v)$, and similarly for the horizontal gradient $\boldsymbol{\nabla}_\perp = (\partial/\partial x, \partial/\partial y)$, the dimensionless system is given by

$$\frac{\partial \boldsymbol{u}_\perp}{\partial t} + (\boldsymbol{u}_\perp \cdot \nabla_\perp)\, \boldsymbol{u}_\perp + w \frac{\partial \boldsymbol{u}_\perp}{\partial \zeta} = -\nabla_\perp p + \frac{1}{Re\alpha^2}\left(\alpha^2 \nabla_\perp^2 \boldsymbol{u}_\perp + \frac{\partial^2 \boldsymbol{u}_\perp}{\partial \zeta^2}\right) + F\hat{\mathbf{e}}_x, \quad (2.4a)$$

$$\frac{\partial w}{\partial t} + (\boldsymbol{u}_\perp \cdot \nabla_\perp)\, w + w\frac{\partial w}{\partial \zeta} = -\frac{1}{\alpha^2}\frac{\partial p}{\partial \zeta} + \frac{b}{Fr^2} + \frac{1}{Re\alpha^2}\left(\alpha^2 \nabla_\perp^2 w + \frac{\partial^2 w}{\partial \zeta^2}\right), \quad (2.4b)$$

$$\nabla_\perp \cdot \boldsymbol{u}_\perp + \frac{\partial w}{\partial \zeta} = 0, \quad (2.4c)$$

$$\frac{\partial b}{\partial t} + (\boldsymbol{u}_\perp \cdot \nabla_\perp)\, b + w\frac{\partial b}{\partial \zeta} + w = \frac{1}{Pe\alpha^2}\left(\alpha^2 \nabla_\perp^2 b + \frac{\partial^2 b}{\partial \zeta^2}\right), \quad (2.4d)$$

where all variables are now non-dimensional and

$$Re = \frac{U^* L^*}{\nu}, \quad Fr = \frac{U^*}{NL^*}, \quad Pe = \frac{U^* L^*}{\kappa} \quad (2.5)$$

are the usual Reynolds, Froude, and Péclet numbers based on the characteristic horizontal scales of the flow. We also note that

$$Pr = \frac{\nu}{\kappa}, \quad \text{so} \quad Pe = PrRe. \quad (2.6)$$

When the stratification is strong, $Fr \ll 1$, and the buoyancy term in the vertical component of the momentum equation is unbalanced unless it is compensated by the vertical pressure gradient. In other words, the flow anisotropy implies that hydrostatic balance must be satisfied at lowest order, which then requires

$$\alpha = Fr, \quad (2.7)$$

implying that the characteristic vertical velocity $W^* = FrU^*$ while the characteristic vertical scale of the flow $H^* = U^*/N$. The scaling for H^* is well-established, and has been observed in several laboratory and numerical experiments (Holford & Linden 1999; Brethouwer *et al.* 2007; Oglethorpe *et al.* 2013).

Keeping only the lowest-order terms in an asymptotic expansion of (2.4) in $\alpha = Fr \ll 1$ yields

$$\frac{\partial \boldsymbol{u}_\perp}{\partial t} + (\boldsymbol{u}_\perp \cdot \nabla_\perp)\, \boldsymbol{u}_\perp + w \frac{\partial \boldsymbol{u}_\perp}{\partial \zeta} = -\nabla_\perp p + \frac{1}{Re_b}\frac{\partial^2 \boldsymbol{u}_\perp}{\partial \zeta^2} + F\hat{\mathbf{e}}_x, \quad (2.8a)$$

$$\frac{\partial p}{\partial \zeta} = b, \qquad \nabla_\perp \cdot \boldsymbol{u}_\perp + \frac{\partial w}{\partial \zeta} = 0, \quad (2.8b,c)$$

$$\frac{\partial b}{\partial t} + (\boldsymbol{u}_\perp \cdot \nabla_\perp)\, b + w\frac{\partial b}{\partial \zeta} + w = \frac{1}{Pe_b}\frac{\partial^2 b}{\partial \zeta^2}, \quad (2.8d)$$

where

$$Re_b = \alpha^2 Re \quad (2.9)$$

is the usually-defined *buoyancy Reynolds number* and

$$Pe_b = PrRe_b = \alpha^2 Pe \quad (2.10)$$

is introduced as the corresponding buoyancy Péclet number. The set of equations (2.8), which will be referred to as the "anisotropically-scaled high-Pe_b" equations hereafter, recovers the results of Billant & Chomaz (2001) and Brethouwer *et al.* (2007). Note that when $Pr = O(1)$, the condition $Re_b \geqslant O(1)$, which is necessary for viscous effects to be small or negligible, implies that $Pe_b = PrRe_b \geqslant O(1)$. As such, the effects of buoyancy diffusion are also small or negligible.

2.2. *Anisotropically-scaled equations for $Pr \ll 1$*

When the Prandtl number is asymptotically small, it is possible that $Pe_b \ll 1 \leqslant Re_b$. In this extreme limit, the diffusion term on the right hand side of (2.4*d*) becomes unbalanced, unless the buoyancy field itself is much smaller than anticipated by the scaling $H^* N^2$ used in the previous section. The strongly diffusive limit has in fact already been studied by Lignières (1999), who showed that the buoyancy equation asymptotically reduces to a balance between the vertical advection of the background stratification and the diffusion of the buoyancy perturbations in that limit. In dimensional terms, we therefore expect $N^2 w^* \simeq \kappa \nabla^2 b^*$. With this in mind, we let $b = Pe_b \hat{b}$ in (2.4*a*)–(2.4*d*) (this is equivalent to scaling the dimensional buoyancy by $\alpha^3 N^2 U^* L^{*2}/\kappa$ instead of $H^* N^2$), and anticipate that $\hat{b} = O(1)$. The resulting dimensionless system becomes

$$\frac{\partial \boldsymbol{u}_\perp}{\partial t} + (\boldsymbol{u}_\perp \cdot \nabla_\perp)\, \boldsymbol{u}_\perp + w \frac{\partial \boldsymbol{u}_\perp}{\partial \zeta} = -\nabla_\perp p + \frac{1}{Re_b}\left(\alpha^2 \nabla_\perp^2 \boldsymbol{u}_\perp + \frac{\partial^2 \boldsymbol{u}_\perp}{\partial \zeta^2}\right) + F\hat{\mathbf{e}}_x, \quad (2.11a)$$

$$\frac{\partial w}{\partial t} + (\boldsymbol{u}_\perp \cdot \nabla_\perp)\, w + w \frac{\partial w}{\partial \zeta} = -\frac{1}{\alpha^2}\frac{\partial p}{\partial \zeta} + \frac{Pe_b}{Fr^2}\hat{b} + \frac{1}{Re_b}\left(\alpha^2 \nabla_\perp^2 w + \frac{\partial^2 w}{\partial \zeta^2}\right), \quad (2.11b)$$

$$\nabla_\perp \cdot \boldsymbol{u}_\perp + \frac{\partial w}{\partial \zeta} = 0, \quad (2.11c)$$

$$\frac{\partial \hat{b}}{\partial t} + (\boldsymbol{u}_\perp \cdot \nabla_\perp)\, \hat{b} + w \frac{\partial \hat{b}}{\partial \zeta} + \frac{1}{Pe_b} w = \frac{1}{Pe_b}\left(\alpha^2 \nabla_\perp^2 \hat{b} + \frac{\partial^2 \hat{b}}{\partial \zeta^2}\right). \quad (2.11d)$$

For sufficiently strong stratification, the vertical component of the momentum equation must again be in hydrostatic balance, which requires

$$\alpha^2 = \frac{Fr^2}{Pe_b} = \frac{Fr^2}{\alpha^2 Pe} \rightarrow \alpha = Fr_M, \text{ where } Fr_M = \left(\frac{Fr^2}{Pe}\right)^{1/4} \quad (2.12)$$

is a modified Froude number (see Lignières 2020; Skoutnev 2023). This scaling implies that the characteristic vertical scale should be $H^* = (Fr^2/Pe)^{1/4} L^*$, and the characteristic vertical velocity scale should be $W^* = (Fr^2/Pe)^{1/4} U^*$.

In the limit $Fr_M \ll 1$ and $Pe_b \ll 1$, keeping only the lowest order terms in (2.11*a*)–(2.11*d*) yields

$$\frac{\partial \boldsymbol{u}_\perp}{\partial t} + (\boldsymbol{u}_\perp \cdot \nabla_\perp)\, \boldsymbol{u}_\perp + w \frac{\partial \boldsymbol{u}_\perp}{\partial \zeta} = -\nabla_\perp p + \frac{1}{Re_b}\frac{\partial^2 \boldsymbol{u}_\perp}{\partial \zeta^2} + F\hat{\mathbf{e}}_x, \quad (2.13a)$$

$$\frac{\partial p}{\partial \zeta} = \hat{b}, \qquad \nabla_\perp \cdot \boldsymbol{u}_\perp + \frac{\partial w}{\partial \zeta} = 0, \qquad w = \frac{\partial^2 \hat{b}}{\partial \zeta^2}. \quad (2.13b,c,d)$$

These equations recover those derived by Skoutnev (2023) albeit using rather different arguments, and are the low Pe_b analogs of equations (2.8). In what follows, we therefore refer to them as the "anisotropically-scaled low-Pe_b" equations.

2.3. *Evidence for multiscale dynamics*

The two sets of anisotropically-scaled equations given by (2.8) for $Pe_b \geqslant O(1)$ and (2.13) for $Pe_b \ll 1$ assume, by construction, that horizontal scales are large, while the vertical scale is small. As such, they necessarily describe the dynamics of *almost* laminar [GPC: I've never been sure about this, as the large scale flow governed by (2.13) itself can be turbulent], weakly-coupled "pancake" vortices or horizontal meanders of the mean flow. They cannot, however, capture the small-scale turbulence that is expected to develop from shear instabilities between these layerwise horizontal motions (Chini *et al.* 2022). Yet, these instabilities are ubiquitous when Re_b is large enough, and have been observed in laboratory experiments, oceanographic *in situ* measurements, as well as direct numerical simulations at $Pr = O(1)$ (XXX need citations each time XXX).

Furthermore, recent DNS of stratified turbulence in the $Pr \ll 1$ low Péclet number regime by Cope *et al.* (2020) also find that flows on small horizontal scales are important. Crucially, their DNS suggest that $H^* \propto (Fr^2/Pe)^{1/3}L^*$ instead of $(Fr^2/Pe)^{1/4}L^*$ and that $W^* \propto (Fr^2/Pe)^{1/6}U^*$ instead of $(Fr^2/Pe)^{1/4}U^*$. These results thus shed some doubt on the relevance of the low-Pe_b anisotropically-scaled equations (2.13) for modeling stratified turbulence, at least at large buoyancy Reynolds number.

In response to these problems, Chini *et al.* (2022) argued that one *must* also take into account the fast, small horizontal scales and study their interaction with the slow, larger-scale anisotropic flow to obtain a more complete and more accurate model of stratified turbulence. Accordingly, they proposed a multiscale asymptotic expansion of the governing equations valid when $Re_b, Pe_b \geqslant O(1)$ and $Fr \ll 1$ (see §3.2 for details) and formally showed that in this limit the governing Boussinesq equations split into a slow/fast quasilinear system; i.e., the small-scale fast dynamics are linear about the slow fields but influence the large-scale slow dynamics through their average turbulent fluxes. When $Pe_b \geqslant O(1)$, which is implicit in their derivation, they find that $H^* = U^*/N$, as in (2.7), consistent with experimental observations of that regime. They also obtain a new scaling for W^* (see § 3.2), which is broadly consistent with DNS data from Maffioli & Davidson (2016).

Encouraged by the success of Chini *et al.* (2022) in modeling stratified turbulence at $Pr = O(1)$, and spurred by the need for an equivalent model at low Pr, we now perform a similar multiscale asymptotic analysis in that limit. The next section first outlines the work of Chini *et al.* (2022) for pedagogical clarity, then extends the analysis to the low Pr regime.

3. Multiscale models for stratified turbulence

We consider the same model set-up as introduced in §2. Here, however, we make no assumption about the amplitude of the vertical flow motions when non-dimensionalising the governing equations, and instead allow it to emerge naturally from the analysis. Accordingly, we non-dimensionalise the vertical velocity by U^*, and correspondingly choose the buoyancy scale to be L^*N^2. Then, the dimensionless system is

$$\frac{\partial \boldsymbol{u}_\perp}{\partial t} + (\boldsymbol{u}_\perp \cdot \nabla_\perp)\,\boldsymbol{u}_\perp + \frac{w}{\alpha}\frac{\partial \boldsymbol{u}_\perp}{\partial \zeta} = -\nabla_\perp p + \frac{1}{Re_b}\left(\alpha^2\nabla_\perp^2 \boldsymbol{u}_\perp + \frac{\partial^2 \boldsymbol{u}_\perp}{\partial \zeta^2}\right) + F\hat{\mathbf{e}}_x, \tag{3.1a}$$

$$\frac{\partial w}{\partial t} + (\boldsymbol{u}_\perp \cdot \nabla_\perp)\, w + \frac{w}{\alpha}\frac{\partial w}{\partial \zeta} = -\frac{1}{\alpha}\frac{\partial p}{\partial \zeta} + \frac{b}{Fr^2} + \frac{1}{Re_b}\left(\alpha^2\nabla_\perp^2 w + \frac{\partial^2 w}{\partial \zeta^2}\right), \tag{3.1b}$$

$$\nabla_\perp \cdot \boldsymbol{u}_\perp + \frac{1}{\alpha}\frac{\partial w}{\partial \zeta} = 0, \tag{3.1c}$$

$$\frac{\partial b}{\partial t} + (\boldsymbol{u}_\perp \cdot \nabla_\perp)\, b + \frac{w}{\alpha}\frac{\partial b}{\partial \zeta} + w = \frac{1}{Pe_b}\left(\alpha^2\nabla_\perp^2 b + \frac{\partial^2 b}{\partial \zeta^2}\right). \tag{3.1d}$$

These equations are the starting point of our analysis. We assume that $Re_b \geqslant O(1)$, and that Fr is sufficiently small to ensure that $\alpha \ll 1$, but make no other *a priori* assumption on the size of Pe_b at this stage.

3.1. *Slow-fast decomposition*

We now perform a multiscale expansion of the system in the limit of small aspect ratio α. Following Chini *et al.* (2022), we assume the existence of two distinct horizontal lengthscales: the original large scales that are $O(1)$ in the nondimensionalization selected, as well as much smaller horizontal scales that are $O(\alpha)$. With that choice, small-scale fluid motions are isotropic by construction. We further assume that the flow has two distinct timescales: a slow timescale associated with the turnover of the large horizontal eddies, as before, and a fast timescale inversely related to the vertical shearing rate of the large-scale mean flow U^*/H^*. In practice, we thus define the slow and fast horizontal coordinates as $\boldsymbol{x}_s = \boldsymbol{x}_\perp$ and $\boldsymbol{x}_f = \boldsymbol{x}_s/\alpha$, respectively (henceforth, the subscript f denotes fast and s denotes slow). Similarly, we split time into slow and fast variables, such that $t_f = t_s/\alpha$ where $t_s = t$. Consequently, the partial derivatives with respect to time and to the horizontal variables become

$$\frac{\partial}{\partial t} = \frac{1}{\alpha}\frac{\partial}{\partial t_f} + \frac{\partial}{\partial t_s}, \qquad \nabla_\perp = \frac{1}{\alpha}\nabla_f + \nabla_s. \tag{3.2}$$

All dependent variables (collectively referred to as q) are now assumed to be functions of both fast and slow length and time scales, so $q = q(\boldsymbol{x}_f, \boldsymbol{x}_s, \zeta, t_f, t_s; \alpha)$.

Assuming the fast and slow scales are sufficiently separated, Chini *et al.* (2022) then define a fast-averaging operator $\overline{(\cdot)}$, such that

$$\overline{q}(\boldsymbol{x}_s, \zeta, t_s; \alpha) = \lim_{T, l_x, l_y \to \infty} \frac{1}{l_x l_y T}\int_0^T \int_D q(\boldsymbol{x}_f, \boldsymbol{x}_s, \zeta, t_f, t_s; \alpha)\mathrm{d}\boldsymbol{x}_f \mathrm{d}t_f, \tag{3.3}$$

where D is a horizontal domain, with fast spatial periods l_x and l_y, and T is the fast time-integration period. With this definition, $\overline{q}$ depends on slow variables only. Each quantity q can then be split into a slowly-varying field $\bar{q}$ and a rapidly fluctuating component $q' = q - \overline{q}$, which implies that the fast-average of the fluctuation field must vanish, i.e., $\overline{q'} = 0$. Note that q' itself could, however, still depend on the slow length and time scales.

We first substitute the expressions (3.2) for $\nabla_\perp$ and $\partial/\partial t$ into in (3.1), and split each quantity q as $\overline{q} + q'$. We then take the fast average of each of the four governing equations to obtain the evolution equation for the mean flow, then subtract the mean from the total to obtain the evolution equation for the fluctuations.

Starting with the continuity equation, we have

$$\frac{1}{\alpha}\nabla_f \cdot \boldsymbol{u'}_\perp + \nabla_s \cdot \bar{\boldsymbol{u}}_\perp + \nabla_s \cdot \boldsymbol{u'}_\perp + \frac{1}{\alpha}\frac{\partial \bar{w}}{\partial \zeta} + \frac{1}{\alpha}\frac{\partial w'}{\partial \zeta} = 0, \tag{3.4}$$

whose fast-average reveals that

$$\nabla_s \cdot \bar{\boldsymbol{u}}_\perp + \frac{1}{\alpha}\frac{\partial \bar{w}}{\partial \zeta} = 0 \tag{3.5a}$$

for the mean flow and

$$\frac{1}{\alpha}\nabla_f \cdot \boldsymbol{u'}_\perp + \nabla_s \cdot \boldsymbol{u'}_\perp + \frac{1}{\alpha}\frac{\partial w'}{\partial \zeta} = 0 \tag{3.5b}$$

for the perturbations.

A similar procedure for the horizontal momentum equation yields

$$\frac{\partial \overline{\boldsymbol{u}}_\perp}{\partial t_s} + \overline{\boldsymbol{u}}_\perp \cdot \nabla_s \overline{\boldsymbol{u}}_\perp + \frac{\overline{w}}{\alpha}\frac{\partial \overline{\boldsymbol{u}}_\perp}{\partial \zeta} + \frac{1}{\alpha}\left(\overline{\boldsymbol{u}'_\perp \cdot \nabla_f \boldsymbol{u}'_\perp + w'\frac{\partial \boldsymbol{u}'_\perp}{\partial \zeta}}\right) + \overline{\boldsymbol{u}'_\perp \cdot \nabla_s \boldsymbol{u}'_\perp}$$
$$= -\nabla_s \overline{p} + \frac{1}{Re_b}\left(\frac{\partial^2 \overline{\boldsymbol{u}}_\perp}{\partial \zeta^2} + \alpha^2 \nabla_s^2 \overline{\boldsymbol{u}}_\perp\right) + \bar{F}, \tag{3.6a}$$

for the mean flow (where $F = \bar{F} = O(1)$ by construction), and

$$\frac{1}{\alpha}\frac{\partial \boldsymbol{u}'_\perp}{\partial t_f} + \frac{\partial \boldsymbol{u}'_\perp}{\partial t_s} + \frac{1}{\alpha}\overline{\boldsymbol{u}}_\perp \cdot \nabla_f \boldsymbol{u}'_\perp + \overline{\boldsymbol{u}}_\perp \cdot \nabla_s \boldsymbol{u}'_\perp + \boldsymbol{u}'_\perp \cdot \nabla_s \overline{\boldsymbol{u}}_\perp + \frac{1}{\alpha}\boldsymbol{u}'_\perp \cdot \nabla_f \boldsymbol{u}'_\perp + \boldsymbol{u}'_\perp \cdot \nabla_s \boldsymbol{u}'_\perp$$
$$+ \frac{1}{\alpha}\left(\overline{w}\frac{\partial \boldsymbol{u}'_\perp}{\partial \zeta} + w'\frac{\partial \overline{\boldsymbol{u}}_\perp}{\partial \zeta} + w'\frac{\partial \boldsymbol{u}'_\perp}{\partial \zeta}\right) = -\frac{1}{\alpha}\nabla_f p' + \frac{1}{Re_b}\left(\nabla_f^2 \boldsymbol{u}'_\perp + \frac{\partial^2 \boldsymbol{u}'_\perp}{\partial \zeta^2}\right) \tag{3.6b}$$

for the fluctuations.

The mean buoyancy equation is

$$\frac{\partial \overline{b}}{\partial t_s} + \overline{\boldsymbol{u}}_\perp \cdot \nabla_s \overline{b} + \frac{\overline{w}}{\alpha}\frac{\partial \overline{b}}{\partial \zeta} + \frac{1}{\alpha}\left(\overline{\boldsymbol{u}'_\perp \cdot \nabla_f b' + w'\frac{\partial b'}{\partial \zeta}}\right) + \overline{\boldsymbol{u}'_\perp \cdot \nabla_s b'} + \overline{w} = \frac{1}{Pe_b}\left(\frac{\partial^2 \overline{b}}{\partial \zeta^2} + \alpha^2 \nabla^2 \overline{b}\right), \tag{3.7a}$$

while the corresponding fluctuation equation becomes:

$$\frac{1}{\alpha}\frac{\partial b'}{\partial t_f} + \frac{\partial b'}{\partial t_s} + \frac{1}{\alpha}\overline{\boldsymbol{u}}_\perp \cdot \nabla_f b' + \boldsymbol{u}'_\perp \cdot \nabla_s \overline{b} + \frac{1}{\alpha}\boldsymbol{u}'_\perp \cdot \nabla_f b' + \boldsymbol{u}'_\perp \cdot \nabla_s b'$$
$$+ \frac{1}{\alpha}\left(w'\frac{\partial \overline{b}}{\partial \zeta} + \overline{w}\frac{\partial b'}{\partial \zeta} + w'\frac{\partial b'}{\partial \zeta}\right) + w' = \frac{1}{Pe_b}\left(\nabla_f^2 b' + \frac{\partial^2 b'}{\partial \zeta^2}\right). \tag{3.7b}$$

Finally, the mean vertical momentum equation is

$$\frac{\partial \overline{w}}{\partial t_s} + \overline{\boldsymbol{u}}_\perp \cdot \nabla_s \overline{w} + \frac{\overline{w}}{\alpha}\frac{\partial \overline{w}}{\partial \zeta} + \frac{1}{\alpha}\left(\overline{\boldsymbol{u}'_\perp \cdot \nabla_f w' + w'\frac{\partial w'}{\partial \zeta}}\right) + \overline{\boldsymbol{u}'_\perp \cdot \nabla_s w'}$$
$$= -\frac{1}{\alpha}\frac{\partial \overline{p}}{\partial \zeta} + \frac{\overline{b}}{Fr^2} + \frac{1}{Re_b}\left(\frac{\partial^2 \overline{w}}{\partial \zeta^2} + \alpha^2 \nabla^2 \overline{w}\right), \tag{3.8a}$$

while the fluctuations satisfy

$$\frac{1}{\alpha}\frac{\partial w'}{\partial t_f} + \frac{\partial w'}{\partial t_s} + \frac{1}{\alpha}\overline{\boldsymbol{u}}_\perp \cdot \nabla_f w' + \boldsymbol{u}'_\perp \cdot \nabla_s \overline{w} + \frac{1}{\alpha}\boldsymbol{u}'_\perp \cdot \nabla_f w' + \boldsymbol{u}'_\perp \cdot \nabla_s w'$$
$$+ \frac{1}{\alpha}\left(w'\frac{\partial \overline{w}}{\partial \zeta} + \overline{w}\frac{\partial w'}{\partial \zeta} + w'\frac{\partial w'}{\partial \zeta}\right) = -\frac{1}{\alpha}\frac{\partial p'}{\partial \zeta} + \frac{b'}{Fr^2} + \frac{1}{Re_b}\left(\nabla_f^2 w' + \frac{\partial^2 w'}{\partial \zeta^2}\right). \tag{3.8b}$$

We see, as noted by Chini *et al.* (2022), that the effective Reynolds and Péclet numbers of the fluctuation equations are Re_b/α and Pe_b/α, respectively, which implies that the fluctuations are formally much *less* viscous and *less* diffusive than the mean.

3.2. *Multiscale model at $Pe_b \geqslant O(1)$*

We begin by summarizing the steps taken by Chini *et al.* (2022) to derive a reduced multiscale model for stratified turbulence at $Re_b, Pe_b \geqslant O(1)$, as most of these steps will be quite similar at low Prandtl number. Following their work, we posit the following asymptotic expansion:

$$[b, p, \boldsymbol{u}_\perp, w] \sim [b_0, p_0, \boldsymbol{u}_{\perp 0}, w_0] + \alpha^{1/2}[b_1, p_1, \boldsymbol{u}_{\perp 1}, w_1] + \alpha[b_2, p_2, \boldsymbol{u}_{\perp 2}, w_2] + \ldots \tag{3.9}$$

The expansion starts at $O(1)$ to reflect the expectation that the dominant contributions to the pressure and the horizontal velocity arise on large horizontal scales. The expansions for b and w also start at $O(1)$ for now, although we readily show below that w_0 and b_0 must both vanish when $\alpha \to 0$. Finally, the expansion proceeds as an asymptotic series in $\alpha^{1/2}$ following the results of Chini *et al.* (2022). They demonstrated (see below for more details) that as the small-scale fluctuations are isotropic, $\boldsymbol{u'}$ and w' are necessarily of the same order. Inspection of the mean horizontal momentum equation then rapidly reveals that both of them need to be $O(\alpha^{1/2})$ to ensure that the Reynolds stresses feed back on $\boldsymbol{u}_{\perp 0}$ at leading-order.

With these choices, we substitute (3.9) into the multiscale equations presented above, working in turn with the continuity equation (3.5), the horizontal component of the momentum equation (3.6), the buoyancy equation (3.7), and finally, the vertical component of the momentum equation (3.8). At each step, we match terms at leading order to infer their sizes and respective evolution equations, and thus derive a reduced model for the flow.

Starting with the mean continuity equation (3.5*a*), we see that the horizontal divergence of the mean flow has to be zero unless $\bar{w}_0 = \bar{w}_1 = 0$. Requiring that this be the case to avoid overly constraining the horizontal flow, we have

$$\nabla_s \cdot \bar{\boldsymbol{u}}_{\perp 0} + \frac{\partial \bar{w}_2}{\partial \zeta} = 0. \tag{3.10a}$$

In the fluctuation continuity equation (3.5*b*), the second term is clearly much smaller than the first and can therefore be neglected from the leading-order expansion. Substituting the asymptotic series (3.9) we then see that

$$\nabla_f \cdot \boldsymbol{u'}_{\perp i} + \frac{\partial w'_i}{\partial \zeta} = 0, \tag{3.10b}$$

for $i = 0, 1$ (for larger values of i, the slow derivative of $\boldsymbol{u'}_{\perp i-2}$ should be taken into account).

We now turn to the mean horizontal component of the momentum equation (3.6*a*). The Reynolds stresses must be $O(1)$ to feedback on the mean flow, so $\boldsymbol{u'}$ and w' must both be $O(\alpha^{1/2})$. Hence, $\boldsymbol{u}'_{\perp 0} = \boldsymbol{0}$ and $w'_0 = 0$, meaning that $\boldsymbol{u}_{\perp 0} = \overline{\boldsymbol{u}}_{\perp 0}$ and that $w_0 = 0$, as both its mean and fluctuating components are zero (see also Chini *et al.* 2022, for a more rigorous discussion of why $\boldsymbol{u}'_{\perp 0} = \boldsymbol{0}$). In the horizontal momentum equation for the fluctuations, the fast dynamics take place at $O(\alpha^{-1/2})$ since $\boldsymbol{u'} = O(\alpha^{1/2})$. Ensuring that pressure comes in at leading order implies that $p'_0 = 0$ so $p_0 = \bar{p}_0$, as expected. Many of the remaining terms are formally higher order, including all fluctuation-fluctuation interactions, which are $O(1)$ or higher. Of the nonlinear terms, the only ones that contribute at leading order are quasilinear: $\alpha^{-1}\overline{\boldsymbol{u}}_\perp \cdot \nabla_f \boldsymbol{u}'_\perp$ and $\alpha^{-1} w' \partial_z \overline{\boldsymbol{u}}_\perp$. We therefore have, after substituting (3.9) in (3.6) and keeping only the leading terms,

$$\frac{\partial \overline{\boldsymbol{u}}_{\perp 0}}{\partial t_s} + \overline{\boldsymbol{u}}_{\perp 0} \cdot \nabla_s \overline{\boldsymbol{u}}_{\perp 0} + \overline{w}_2 \frac{\partial \overline{\boldsymbol{u}}_{\perp 0}}{\partial \zeta} = -\nabla_s \overline{p}_0 - \frac{\partial}{\partial \zeta}\left(\overline{w'_1 \boldsymbol{u}'_{\perp 1}}\right) + \frac{1}{Re_b}\frac{\partial^2 \overline{\boldsymbol{u}}_{\perp 0}}{\partial \zeta^2} + \overline{F}, \tag{3.11a}$$

$$\frac{\partial \boldsymbol{u}'_{\perp 1}}{\partial t_f} + \overline{\boldsymbol{u}}_{\perp 0} \cdot \nabla_f \boldsymbol{u}'_{\perp 1} + w'_1 \frac{\partial \overline{\boldsymbol{u}}_{\perp 0}}{\partial \zeta} = -\nabla_f p'_1 + \frac{\alpha}{Re_b}\left(\nabla_f^2 \boldsymbol{u}'_{\perp 1} + \frac{\partial^2 \boldsymbol{u}'_{\perp 1}}{\partial \zeta^2}\right). \tag{3.11b}$$

where the viscous term in the fluctuation equation was kept to regularize it, but is formally higher order.

Next, we examine the buoyancy equation, which reveals the sizes of $\bar{b}$ and b'. In the mean equation (3.7*a*), $\bar{w} = O(\alpha)$, and the buoyancy flux term is formally also of that order (see Chini *et al.* 2022, and also below). This shows that $\bar{b} = O(\alpha)$ as well, as long as $Pe_b \geqslant O(1)$, which is implicit in the regime considered in this section, and implies $\bar{b}_0 = \bar{b}_1 = 0$. To confirm the size of the buoyancy flux, we inspect the buoyancy fluctuation equation (3.7*b*). In order to be in a regime where the stratification impacts the turbulent motions, the $O(b'/\alpha)$ fast dynamics must be of the same order as the advection of the background stratification, which is $O(w') = O(\alpha^{1/2})$. This implies that $b' = O(\alpha^{3/2})$, so $b'_0 = b'_1 = b'_2 = 0$. With that choice, $b_0 = b_1 = 0$, and $b_2 = \bar{b}_2$. Fluctuation-fluctuation interactions in this equation are again formally higher order, and the only remaining nonlinearities are quasilinear. At leading order, using (3.9) in (3.7) shows that the mean and fluctuation buoyancy equations are

$$\frac{\partial \bar{b}_2}{\partial t_s} + \overline{\boldsymbol{u}}_{\perp 0} \cdot \nabla_s \bar{b}_2 + \overline{w}_2 \frac{\partial \bar{b}_2}{\partial \zeta} + \overline{w}_2 = -\frac{\partial}{\partial \zeta}\left(\overline{w'_1 b'_3}\right) + \frac{1}{Pe_b}\frac{\partial^2 \bar{b}_2}{\partial \zeta^2}, \tag{3.12a}$$

$$\frac{\partial b'_3}{\partial t_f} + \overline{\boldsymbol{u}}_{\perp 0} \cdot \nabla_f b'_3 + w'_1 \frac{\partial \bar{b}_2}{\partial \zeta} + w'_1 = \frac{\alpha}{Pe_b}\left(\nabla_f^2 b'_3 + \frac{\partial^2 b'_3}{\partial \zeta^2}\right). \tag{3.12b}$$

where as before the diffusion term in the fluctuation equation was added to regularize it.

Finally, we use the information gathered so far regarding $\bar{b}$ and b' to deduce the leading order asymptotic terms in the vertical component of the momentum equation. In the mean equation (3.8*a*), a hydrostatic leading-order balance requires $\alpha = Fr$, as in the anisotropically-scaled model described in Section 2.1. This specification, when applied to the fluctuation equation (3.8*b*), is quite satisfactory as it implies that the fluctuating buoyancy force b'/Fr^2 arises at leading order, as desired. It can also easily be shown that, once again, fluctuation-fluctuation interactions are negligible at leading order, so the fast dynamics are quasilinear. Substituting (3.9) in (3.8) and using all of the information available, we obtain the leading order mean and fluctuating components of the vertical momentum equation

$$\frac{\partial \overline{p}_0}{\partial \zeta} = \bar{b}_2, \tag{3.13a}$$

$$\frac{\partial w'_1}{\partial t_f} + \overline{\boldsymbol{u}}_{\perp 0} \cdot \nabla_f w'_1 = -\frac{\partial p'_1}{\partial \zeta} + b'_3 + \frac{\alpha}{Re_b}\left(\nabla_f^2 w'_1 + \frac{\partial^2 w'_1}{\partial \zeta^2}\right). \tag{3.13b}$$

where the formally higher-order viscous term was added to regularize the fluctuation equation.

The system of equations formed by (3.10) (with $i = 1$), (3.11), (3.12) and (3.13), is equivalent to equations (2.28-2.35) in Chini *et al.* (2022), the main difference simply arising from a different choice of non-dimensionalization. These equations are fully closed, and therefore self-consistent. Crucially, the fluctuation equations are quasilinear.

These equations are valid whenever $\alpha \ll 1$ (equivalently, $Fr \ll 1$ since $\alpha = Fr$), and the buoyancy Reynolds and Péclet numbers are both $O(1)$ or larger, thus allowing for the growth and saturation of the fluctuations via interactions with the mean. When $Pr = O(1)$, $Re_b \geqslant O(1)$ necessarily implies $Pe_b \geqslant O(1)$, so the two conditions are equivalent. Since $Re_b = \alpha^2 Re$, this condition is equivalent to $Re, Pe \geqslant O(Fr^{-2})$.

For low Pr, these reduced equations remain valid as long as $Re_b, Pe_b \geqslant O(1)$. However, for *sufficiently* low Pr it is possible to have an intermediate regime where $Re_b \geqslant O(1)$ while $Pe_b = PrRe_b \ll 1$, and that regime is *not* captured by the Chini *et al.* (2022) equations. Yet, it is likely relevant in stellar interiors, where Pr is asymptotically small (Garaud *et al.* 2015*b*). We now perform a similar analysis to develop a multiscale model that is valid for low Pe_b flows.

3.3. *Multiscale model for $Pe_b \ll 1$*

In the limit of small Pe_b, the arguments presented above continue to apply for the continuity equation and the horizontal component of the momentum equation, neither of which involve buoyancy terms. However, the procedure subsequently fails because diffusive effects dominate in the buoyancy equation and are unbalanced unless b is much smaller than expected, mirroring the argument made in Section 2.2. To capture this correctly within the context of our proposed multiscale model, we must introduce a two-parameter expansion for small α *and* small Pe_b in lieu of (3.9).

As in Chini *et al.* (2022), we assume that the asymptotic series in α proceeds in powers of $\alpha^{1/2}$, and show the self-consistency of this choice below. Inspired by Lignières (1999), we now also assume that each quantity can be expanded as a series in powers of Pe_b as well. We therefore have

$$q = q_{00} + \alpha^{1/2} q_{01} + \alpha\, q_{02} + \dots + Pe_b \left(q_{10} + \alpha^{1/2} q_{11} + \alpha\, q_{12} + \dots \right) + O(Pe_b^2), \quad (3.14)$$

for $q \in \{\boldsymbol{u}_\perp, p, w, b\}$ and assume that $\bar{\boldsymbol{u}}_{\perp 00} = O(1)$ and $\bar{p}_{00} = O(1)$ to match the forcing. We then proceed exactly as before, substituting (3.14) in turn into the multiscale continuity equation (3.5), the horizontal component of the momentum eqation (3.6), the buoyancy equation (3.7), and the vertical component of the momentum equation (3.8), to extract the relevant reduced equations at leading order.

Starting with the mean continuity equation (3.5a), we find again that $\overline{w} = O(\alpha)$ and hence $\overline{w}_{00} = \overline{w}_{01} = 0$. Equation (3.5$b$) further implies that $O(\boldsymbol{u}'_\perp) = O(w')$, so

$$\nabla_s \cdot \overline{\boldsymbol{u}}_{\perp 00} + \frac{\partial \overline{w}_{02}}{\partial \zeta} = 0, \quad (3.15a)$$

$$\nabla_f \cdot \boldsymbol{u}'_{\perp 01} + \frac{\partial w'_{01}}{\partial \zeta} = 0. \quad (3.15b)$$

From the mean horizontal component of the momentum equation (3.6a), $\boldsymbol{u'}_\perp$ and w' must both be $O(\alpha^{1/2})$ as before, hence $\boldsymbol{u}'_{\perp 00} = 0$ and $w'_{00} = 0$, so $\boldsymbol{u}_{\perp 00} = \overline{\boldsymbol{u}}_{\perp 00}$ and $w_{00} = 0$. The inferred sizes of the velocity fluctuations mean that fluctuation-fluctuation interactions are again formally higher-order, and the only remaining nonlinearities in the corresponding fluctuation equation (3.6b) are quasilinear. Finally, for the fluctuating horizontal pressure gradient to influence the fluctuations of horizontal velocity at leading order requires $p' = O(\boldsymbol{u}'_\perp) = O(\alpha^{1/2})$, hence $p'_{00} = 0$. Substituting (3.14) into (3.6a) and (3.6b), using the information available, and keeping only the lowest-order terms, shows that

$$\frac{\partial \overline{\boldsymbol{u}}_{\perp 00}}{\partial t_s} + (\overline{\boldsymbol{u}}_{\perp 00} \cdot \nabla_s) \overline{\boldsymbol{u}}_{\perp 00} + \overline{w}_{02} \frac{\partial \overline{\boldsymbol{u}}_{\perp 00}}{\partial \zeta} = -\nabla_s \overline{p}_{00} - \frac{\partial}{\partial \zeta} \left(\overline{w'_{01} \boldsymbol{u}'_{\perp 01}} \right) + \frac{1}{Re_b} \frac{\partial^2 \overline{\boldsymbol{u}}_{\perp 00}}{\partial \zeta^2} + F \hat{\mathbf{e}}_x, \quad (3.16a)$$

$$\frac{\partial \boldsymbol{u}'_{\perp 01}}{\partial t_f} + (\overline{\boldsymbol{u}}_{\perp 00} \cdot \nabla_f) \boldsymbol{u}'_{\perp 01} + w'_{01} \frac{\partial \overline{\boldsymbol{u}}_{\perp 00}}{\partial \zeta} = -\nabla_f p'_{01} + \frac{\alpha}{Re_b} \left(\nabla_f^2 \boldsymbol{u}'_{\perp 01} + \frac{\partial^2 \boldsymbol{u}'_{\perp 01}}{\partial \zeta^2} \right), \quad (3.16b)$$

where the viscous term in the fluctuation equation was added to regularize it, as usual.

Thus far, each step in the analysis has been identical to that taken in the previous section. Rapid diffusion, however, affects the size of the mean and fluctuating buoyancy fields $\bar{b}$ and b', and does so in different ways because the effective Péclet number of the fluctuations is larger than that of the mean flow. More specifically, having assumed in this section that $Pe_b \ll 1$, we see that two possibilities arise when $\alpha \ll 1$: either $\alpha \ll Pe_b \ll 1$, in which case diffusion is dominant in the mean buoyancy equation but negligible in the fluctuation buoyancy equation, or $Pe_b \ll \alpha$ in which case diffusion is dominant at all scales. In what follows, we investigate both cases in turn.

Before doing so, however, we note that the mean buoyancy equation (3.7a) in both cases is unbalanced unless $\bar{b} = O(\alpha Pe_b)$ to match the $\bar{w}$ term (again mirroring the arguments given in Section 2.2). This implies $\bar{b}_{0i} = 0$, $\forall i$, and $\bar{b}_{10} = \bar{b}_{11} = 0$. At lowest order in Pe_b, the only remaining terms from (3.7a) are therefore

$$\frac{1}{\alpha}\left(\overline{\boldsymbol{u}'_\perp \cdot \nabla_f b' + w'\frac{\partial b'}{\partial \zeta}}\right) + \bar{w} = \frac{1}{Pe_b}\frac{\partial^2 \bar{b}}{\partial \zeta^2}, \tag{3.17}$$

where the size of b' is yet to be determined, and differs depending on the relative sizes of Pe_b and α. For this reason, we have retained the turbulent buoyancy flux for now.

3.3.1. *Case 1: $\alpha \ll Pe_b \ll 1$ (the intermediate regime)*

We first consider a regime where $\alpha \ll Pe_b \ll 1$ and henceforth refer to this configuration as the "intermediate regime". While diffusion dominates the mean buoyancy equation, the fact that $\alpha/Pe_b \ll 1$ implies that it only formally enters the buoyancy fluctuation equation (3.7b) at higher order. Because of this, the evolution of b' is very similar to that obtained in Chini *et al.* (2022). As in §3.2, we ensure that the background stratification influences the fast dynamics of b' by requiring $b'/\alpha = O(w') = O(\alpha^{1/2})$, so $b' = O(\alpha^{3/2})$. This implies that $b'_{00}, b'_{01}, b'_{02} = 0$, but $b'_{03} \neq 0$.

Substituting the ansatz (3.14) into the mean and fluctuation buoyancy equations and using the information collected so far we therefore have

$$\frac{\partial}{\partial \zeta}\left(\overline{w'_{01}b'_{03}}\right) + \bar{w}_{02} = \frac{\partial^2 \bar{b}_{12}}{\partial \zeta^2}, \tag{3.18a}$$

$$\frac{\partial b'_{03}}{\partial t_f} + \bar{\boldsymbol{u}}_{\perp 00} \cdot \nabla_f b'_{03} + w'_{01} \quad = \frac{\alpha}{Pe_b}\left(\nabla_f^2 b'_{03} + \frac{\partial^2 b'_{03}}{\partial \zeta^2}\right), \tag{3.18b}$$

where the diffusion term for the fluctuations was kept to regularize the equation, but is formally higher order.

We note that the reduced buoyancy fluctuation equation in this regime differs slightly from the one derived by Chini *et al.* (2022) given in (3.12b), because it does not contain a term of the form $w'_{01}\partial\bar{b}/\partial\zeta$, which is formally higher-order when $Pe_b \ll 1$. Also, we see that the mean buoyancy equation in that regime is a little different from the asymptotic Low Péclet Number (LPN) equations of Lignières (1999), which would not contain a turbulent flux term. This discrepancy arises because his derivation assumes that all dynamics are diffusive, whereas in this intermediate regime the fluctuation dynamics are not and can therefore influence the mean buoyancy field at leading order.

Finally, we examine the vertical component of the momentum equation. Based on past experience in the $Pe_b \geqslant O(1)$ case (see Section 3.2), one would naively expect to recover hydrostatic equilibrium at leading order in the mean vertical momentum equation (3.8a). Because $\bar{b} = O(\alpha Pe_b)$, this would imply $\alpha = (Fr^2/Pe_b)^{1/2}$ as in the low Pe_b anisotropically-scaled equations of Section 2.2. However, that choice leads to an irreconcilable inconsistency in the fluctuation equation (3.8b): the fluctuation pressure gradient term is $O(\alpha^{-1/2})$, as are the fast inertial dynamics of w', but the fluctuation buoyancy term is $O(\alpha^{3/2}/Fr^2) = O(\alpha^{-1/2}/Pe_b)$, which is formally much larger than any other term, and is therefore unbalanced. In order words, we cannot reconcile hydrostatic equilibrium at leading order for the mean flow with a balanced equation for the fluctuation w'.

The solution to this conundrum is to insist instead that the w' equation be balanced, in which case we must have $O(\alpha^{-1/2}) = O(\alpha^{3/2}Fr^{-2})$, and thus recover the standard scaling relationship $\alpha = Fr$ (Billant & Chomaz 2001; Brethouwer *et al.* 2007; Chini *et al.* 2022). With this choice, we are forced to require that the leading-order vertical pressure gradient in the mean equation be zero or otherwise be unbalanced. This perhaps surprising result is discussed in §4 below. Substituting (3.14) in (3.8), we obtain the reduced mean and fluctuating vertical component of the momentum equation at leading order,

$$\frac{\partial \bar{p}_{00}}{\partial \zeta} = 0, \tag{3.19a}$$

$$\frac{\partial w'_{01}}{\partial t_f} + \overline{\boldsymbol{u}}_{\perp 00} \cdot \nabla_f w'_{01} = -\frac{\partial p'_{01}}{\partial \zeta} + b'_{03} + \frac{\alpha}{Re_b}\left(\nabla_f^2 w'_{01} + \frac{\partial^2 w'_{01}}{\partial \zeta^2}\right), \tag{3.19b}$$

where the higher-order viscous term is added to regularize the fluctuation equation.

The set of equations formed by (3.15), (3.16), (3.18), and (3.19) are the intermediate regime analogs of the Chini *et al.* (2022) reduced model. They are valid as long as $Re_b \geqslant O(1)$, and $\alpha \ll Pe_b \ll 1$. Given that $\alpha = Fr$ in this regime, this is equivalent to requiring that $Fr \ll 1$ (so $\alpha \ll 1$), $Re \geqslant Fr^{-2}$, and $Fr^{-1} \ll Pe \ll Fr^{-2}$. The physical implication of these equations, and their potential caveats, are discussed in §4.

3.3.2. *Case 2: $Pe_b \ll \alpha$ (the fully diffusive regime)*

We now consider the regime where $Pe_b \ll \alpha$, in which both mean and fluctuating buoyancy fields are dominated by diffusion. We refer to this hereafter as the fully diffusive regime. Inspection of (3.7b) shows that the diffusion term in the fluctuation equation is unbalanced unless $b' = O(Pe_b w')$. We previously found that the vertical velocity fluctuations are $O(\alpha^{1/2})$, which implies here that $b' = O(\alpha^{1/2}Pe_b)$. We conclude that $b'_{0i} = 0\ \forall i$, and that $b'_{10} = 0$ as well. Combined with the results obtained earlier for the mean buoyancy equation in the diffusive limit, we conclude that $b_{10} = 0$ while $b_{11} = b'_{11}$.

Using this information and substituting (3.14) into (3.7), we obtain at lowest order

$$\overline{w}_{02} = \frac{\partial^2 \overline{b}_{12}}{\partial \zeta^2}, \tag{3.20a}$$

$$w'_{01} = \nabla_f^2 b'_{11} + \frac{\partial^2 b'_{11}}{\partial \zeta^2}, \tag{3.20b}$$

which is as expected from the LPN dynamics central to this regime (Lignières 1999). The buoyancy equation is linear and does not contain any time dependence, instead instantaneously coupling the vertical velocity and buoyancy fields to one another. The validity of Lignières' LPN equations was verified numerically by Cope *et al.* (2020), for instance.

As usual, the last step of the derivation involves the vertical component of the momentum equation. As in Section 3.3.1, requiring hydrostatic equilibrium for the mean flow would imply $\alpha^2 = Fr^2/Pe_b$ (Lignières 2020; Skoutnev 2023), but leads to an inconsistency in the fluctuation equation, where the buoyancy term would be unbalanced. To see this, note that $b'/Fr^2 = O(\alpha^{1/2}Pe_b/Fr^2) = O(\alpha^{-3/2})$ with that choice for α, while the fluctuating pressure term (and all other dominant terms in the equation) is only $O(\alpha^{-1/2})$. As in the previous section, the resolution is to insist that the buoyancy term in the fluctuation equation should be balanced instead. Here, this implies

$$O\left(\frac{p'}{\alpha}\right) = O\left(\frac{b'}{Fr^2}\right) \rightarrow \alpha = \frac{Fr^2}{Pe_b} \tag{3.21}$$

using the fact that $p' = O(\alpha^{1/2})$ and $b' = O(\alpha^{1/2}Pe_b)$. Recalling that $Pe_b = \alpha^2 Pe$, we then recover the crucial scaling relationship

$$\alpha = \left(\frac{Fr^2}{Pe}\right)^{1/3} = Fr_M^{4/3}, \tag{3.22}$$

which had originally been proposed by Cope *et al.* (2020) based on their DNS data. This study has therefore found a sound theoretical basis for their empirical results.

After substituting (3.14) into (3.8) and using the available information, we obtain

$$\frac{\partial \bar{p}_{00}}{\partial \zeta} = 0, \tag{3.23a}$$

$$\frac{\partial w'_{01}}{\partial t_f} + (\overline{\boldsymbol{u}}_{\perp 00} \cdot \nabla_f) w'_{01} = -\frac{\partial p'_{01}}{\partial \zeta} + b'_{11} + \frac{\alpha}{Re_b}\left(\nabla_f^2 w'_{01} + \frac{\partial^2 w'_{01}}{\partial \zeta^2}\right), \tag{3.23b}$$

which is very similar to the system obtained in the intermediate regime studied in Section 3.3.1, except of the appearance of the buoyancy fluctuation term b'_{11} instead of b'_{03}. As before, formally higher-order viscous terms are kept to regularize the fluctuation equation.

The set of equations formed by (3.15), (3.16), (3.20), and (3.23) are the fully-diffusive regime analogs of the Chini *et al.* (2022) reduced model. They are valid as long as $Re_b \geqslant O(1)$, and $Pe_b \ll \alpha \ll 1$. Given that $\alpha = (Fr^2/Pe)^{1/3}$ in this regime, this is equivalent to requiring that $Fr^2 \ll Pe$ (to ensure $\alpha \ll 1$), $Pe \ll Fr^{-1}$ (to ensure $Pe_b \ll \alpha$), and $Pe \geqslant Pr^3 Fr^{-4}$ (to ensure that $Re_b \geqslant O(1)$). The three conditions combined create a triangle in logarithmic parameter space in which the equations are valid – see §4.2. As an important self-consistency check, we see that the $Pe_b = \alpha$ transition between the fully diffusive regime and the intermediate regime is the same ($Pe = Fr^{-1}$) regardless of the direction one approaches it from.

The physical implication of these equations, and their potential caveats, are discussed in §4.

4. Discussion

In this work, we have expanded the work of Chini *et al.* (2022) to perform a multiscale asymptotic analysis of stratified turbulence at low Prandtl number. Our work demonstrates the existence of several different regimes depending on the strength of the stratification (quantified by the inverse Froude number) and the rate of buoyancy diffusion (quantified by the inverse Péclet number). In each regime, the asymptotic analysis self-consistently reveals a slow-fast system of quasilinear equations describing the concurrent evolution of a highly anisotropic, slow, large-scale mean flow and isotropic, fast, small-scale fluctuations. The large-scale anisotropy is characterized by the aspect ratio α (the ratio of the vertical to horizontal large scales), whose functional dependence on Fr and Pe naturally emerges from the analysis. The various regime boundaries are locations in parameter space where relevant Reynolds and Péclet numbers for the mean flow and fluctuation equations are $O(1)$, signifying transitions between viscous vs. non-viscous dynamics, and/or diffusive vs. non-diffusive dynamics. We now summarize our findings in each regime, before discussing the model assumptions as well as the implications of our results for low Prandtl number fluids.

4.1. *Synopsis of multiscale equations and their validity*

The first regime is characterized by $Fr \ll 1$ and $Pe_b, Re_b \geqslant O(1)$, where $Re_b = \alpha^2 Re$ and $Pe_b = \alpha^2 Pe$. In this regime, we recover the reduced model of Chini *et al.* (2022) exactly, and $\alpha = Fr$. Recalling that at leading order, $w'_1 = w'/\alpha^{1/2}$, $b'_3 = b'/\alpha^{3/2}$ (and similarly for all other dependent variables), that $\partial/\partial t_f = \alpha\partial/\partial t$ (and similarly for ∇_f and $\nabla_\perp$), and finally that $\partial/\partial\zeta = \alpha\partial/\partial z$, we can rewrite (3.10), (3.11), (3.12) and (3.13) into the following quasilinear system for mean and fluctuations, expressed in the original isotropic single-scale variables:

Mean flow equations:

$$\frac{\partial \overline{\boldsymbol{u}}_\perp}{\partial t} + \overline{\boldsymbol{u}}_\perp \cdot \nabla \overline{\boldsymbol{u}}_\perp = -\nabla_\perp \overline{p} - \frac{\partial}{\partial z}\left(\overline{w'\boldsymbol{u}'_\perp}\right) + \frac{1}{Re}\frac{\partial^2 \overline{\boldsymbol{u}}_\perp}{\partial z^2} + \bar{F}\hat{\mathbf{e}}_x, \tag{4.1a}$$

$$\frac{\partial \overline{p}}{\partial z} = \frac{\bar{b}}{Fr^2}, \qquad \nabla \cdot \overline{\boldsymbol{u}} = 0, \tag{4.1b}$$

$$\frac{\partial \bar{b}}{\partial t} + \overline{\boldsymbol{u}}_\perp \cdot \nabla \bar{b} + \overline{w} = -\frac{\partial}{\partial z}\left(\overline{w'b'}\right) + \frac{1}{Pe}\frac{\partial^2 \bar{b}}{\partial z^2}. \tag{4.1c}$$

Fluctuation equations:

$$\frac{\partial \boldsymbol{u}'_\perp}{\partial t} + \overline{\boldsymbol{u}}_\perp \cdot \nabla_\perp \boldsymbol{u}'_\perp + w'\frac{\partial \overline{\boldsymbol{u}}_\perp}{\partial z} = -\nabla_\perp p' + \frac{1}{Re}\nabla^2 \boldsymbol{u}'_\perp, \tag{4.1d}$$

$$\frac{\partial w'}{\partial t} + \overline{\boldsymbol{u}}_\perp \cdot \nabla_\perp w' = -\frac{\partial p'}{\partial z} + \frac{b'}{Fr^2} + \frac{1}{Re}\nabla^2 w', \tag{4.1e}$$

$$\nabla \cdot \boldsymbol{u}' = 0, \tag{4.1f}$$

$$\frac{\partial b'}{\partial t} + \overline{\boldsymbol{u}}_\perp \cdot \nabla_\perp b' + w'\frac{\partial \bar{b}}{\partial z} + w' = \frac{1}{Pe}\nabla^2 b'. \tag{4.1g}$$

This system is exactly equivalent to equations (2.28-2.35) in Chini *et al.* (2022). It is valid when $Fr \ll 1$, and $Re, Pe \geqslant O(Fr^{-2})$, which corresponds to $Re_b, Pe_b \geqslant O(1)$. The advantage of re-casting the equations back in the original isotropic variables is now readily apparent: the system has the exact form one often has to *assume* when making a quasilinear approximation (XXX maybe cite some references here? Not sure what a good one would be XXX) (KS: Brad Marston's papers could be options here). However, through this work we have demonstrated that this form is in fact a natural outcome of the slow-fast asymptotic expansion, and is therefore formally exact at this order.

Dimensionally, this regime has a characteristic vertical scale $H^* = \alpha L^* = U^*/N$. The characteristic vertical velocity is $W^* = \alpha^{1/2}U^* = (U^{*3}/NL^*)^{1/2}$, and w dominated by small-scale fluctuations. The characteristic buoyancy scale is N^2H^* and b is dominated by large scales. Note that the characteristic horizontal velocity always has amplitude U^* and is primarily large scale, by assumption. These findings have been validated in numerical and laboratory experiments (Holford & Linden 1999; Brethouwer *et al.* 2007; Oglethorpe *et al.* 2013; Maffioli & Davidson 2016). XXX Colm, are there other obvious references we should cite?

The case where $Fr \ll 1$, $Re_b \geqslant O(1)$ and $\alpha \ll Pe_b \ll 1$ is an intermediate regime where the mean flow is diffusive, while the fluctuations are not. In this regime, we also have $\alpha = Fr$, and the slow-fast system of equations (3.15), (3.16), (3.18), and (3.19), similarly expressed in the original isotropic single-scale variables, becomes the following quasilinear system:

Mean flow equations:

$$\frac{\partial \overline{\boldsymbol{u}}_\perp}{\partial t} + \overline{\boldsymbol{u}}_\perp \cdot \nabla \overline{\boldsymbol{u}}_\perp = -\nabla_\perp \overline{p} - \frac{\partial}{\partial z}\left(\overline{w' \boldsymbol{u}'_\perp}\right) + \frac{1}{Re}\frac{\partial^2 \overline{\boldsymbol{u}}_\perp}{\partial z^2} + \bar{F}\hat{\mathbf{e}}_x, \tag{4.2a}$$

$$\frac{\partial \overline{p}}{\partial z} = 0, \qquad \nabla \cdot \overline{\boldsymbol{u}} = 0, \tag{4.2b,c}$$

$$\overline{w} = -\frac{\partial}{\partial z}\left(\overline{w' b'}\right) + \frac{1}{Pe}\frac{\partial^2 \overline{b}}{\partial z^2}. \tag{4.2d}$$

Fluctuation equations:

$$\frac{\partial \boldsymbol{u}'_\perp}{\partial t} + \overline{\boldsymbol{u}}_\perp \cdot \nabla_\perp \boldsymbol{u}'_\perp + w' \frac{\partial \overline{\boldsymbol{u}}_\perp}{\partial z} = -\nabla_\perp p' + \frac{1}{Re}\nabla^2 \boldsymbol{u}'_\perp, \tag{4.2b}$$

$$\frac{\partial w'}{\partial t} + \overline{\boldsymbol{u}}_\perp \cdot \nabla_\perp w' = -\frac{\partial p'}{\partial z} + \frac{b'}{Fr^2} + \frac{1}{Re}\nabla^2 w', \tag{4.2c}$$

$$\nabla \cdot \boldsymbol{u}' = 0, \tag{4.2d}$$

$$\frac{\partial b'}{\partial t} + \overline{\boldsymbol{u}}_\perp \cdot \nabla_\perp b' + w' = \frac{1}{Pe}\nabla^2 b'. \tag{4.2e}$$

This system is valid while $Re \geqslant Fr^{-2}$ (so $Re_b \geqslant O(1)$), and $Fr^{-1} \ll Pe \ll Fr^{-2}$ (so $\alpha \ll Pe_b \ll 1$). By writing the equations back in the original isotropic variables, we now see that the correct quasilinear equations at this order are almost the same as in the Chini *et al.* (2022) regime, except that terms in $\overline{b}$ are dropped (in the mean hydrostatic balance and in the buoyancy perturbation equation) because they are formally of higher order. In addition, the mean buoyancy equation takes the LPN form of Lignières *et al.* (1999), modified by the fluctuation-induced buoyancy flux.

Dimensionally, the same conclusions are reached for the vertical lengthscale and vertical velocity scale as above. However, the buoyancy field is now dominated by large scales if $Pe_b \geqslant \alpha^{1/2}$, and by small scales if $Pe_b \leqslant \alpha^{1/2}$. Testing these scaling laws numerically will be very difficult, unfortunately, because the range of the intermediate region is very small (holding Pe constant while varying Fr^{-1} or vice-versa) unless Pr is itself very small.

Finally, the case where $Fr \ll 1$, $Re_b \geqslant O(1)$ and $Pe_b \ll \alpha$ corresponds to a fully diffusive regime where both mean flow and fluctuations are dominated by diffusion and reduce to the LPN balance derived by Lignières (1999). In this case, we have demonstrated that $\alpha = (Fr^2/Pe)^{1/3}$. When written in the original isotropic, single-scale variables, the slow-fast system of equations (3.15), (3.16), (3.20), and (3.23) becomes

Mean flow equations:

$$\frac{\partial \overline{\boldsymbol{u}}_\perp}{\partial t} + \overline{\boldsymbol{u}}_\perp \cdot \nabla \overline{\boldsymbol{u}}_\perp = -\nabla_\perp \overline{p} - \frac{\partial}{\partial z}\left(\overline{w' \boldsymbol{u}'_\perp}\right) + \frac{1}{Re}\frac{\partial^2 \overline{\boldsymbol{u}}_\perp}{\partial z^2} + \bar{F}\hat{\mathbf{e}}_x, \tag{4.3a}$$

$$\frac{\partial \overline{p}}{\partial z} = 0, \qquad \nabla \cdot \overline{\boldsymbol{u}} = 0, \tag{4.3b,c}$$

$$\overline{w} = \frac{1}{Pe}\frac{\partial^2 \overline{b}}{\partial z^2}. \tag{4.3d}$$

Fluctuation equations:

$$\frac{\partial \boldsymbol{u}'_\perp}{\partial t} + \overline{\boldsymbol{u}}_\perp \cdot \nabla_\perp \boldsymbol{u}'_\perp + w' \frac{\partial \overline{\boldsymbol{u}}_\perp}{\partial z} = -\nabla_\perp p' + \frac{1}{Re}\nabla^2 \boldsymbol{u}'_\perp, \tag{4.3b}$$

$$\frac{\partial w'}{\partial t} + \overline{\boldsymbol{u}}_\perp \cdot \nabla_\perp w' = -\frac{\partial p'}{\partial z} + \frac{b'}{Fr^2} + \frac{1}{Re}\nabla^2 w', \tag{4.3c}$$

$$\nabla \cdot \boldsymbol{u}' = 0, \tag{4.3d}$$

$$w' = \frac{1}{Pe}\nabla^2 b'. \tag{4.3e}$$

This system is valid while $Re_b \geqslant O(1)$, and $Pe_b \ll \alpha \ll 1$. As $\alpha = (Fr^2/Pe)^{1/3}$, this is equivalent to $Fr^2 \ll Pe$ (such that $\alpha \ll 1$), $Pe \ll Fr^{-1}$ (such that $Pe_b \ll \alpha$), and $Pe \geqslant Pr^3 Fr^{-4}$ (such that $Re_b \geqslant O(1)$). When written in the isotropic variables, we see that the slow-fast expansion naturally recovers what one would expect a quasilinear expansion of the LPN equations of Lignières (1999) to look like.

Dimensionally, the characteristic vertical scale in this regime is $H^* = \alpha L^* = (Fr^2/Pe)^{1/3} L^* = (U^* \kappa / N^2)^{1/3}$. The characteristic vertical velocity is $W^* = \alpha^{1/2} U^* = (Fr^2/Pe)^{1/6} U^* = (U^{*7}\kappa / N^2 L^{*3})^{1/6}$, and is dominated by small-scale fluctuations. The characteristic buoyancy scale is $Pe(Fr^2/Pe)^{5/6} L^* N^2 = (U^{*11/6}\kappa^{-1/6} N^{-5/3} L^{*-3/2}) L^* N^2$ and is dominated by small-scale fluctuations as well. These scalings have been validated by the DNS of Cope *et al.* (2020).

Crucially, we find that in all three regimes the characteristic vertical velocity $W^* = \alpha^{1/2} U^*$ is significantly larger than what is predicted from the anisotropically scaled equations of §2.1 and §2.2 where $W^* = \alpha U^*$. This has implications for turbulent vertical transport of buoyancy and passive scalars in stellar interiors (see §5).

Finally, note that in all of these regimes, we have assumed $Re_b \geqslant O(1)$ which then implies that $Re_b \gg \alpha$ since $\alpha \ll 1$. Recalling that the fluctuation equations have an effective Reynolds number Re_b/α, this condition is necessary to ensure that the small-scale fluctuations can develop without being suppressed by viscosity, and is therefore key to the multiscale expansions derived here. When $Re_b \leqslant O(1)$, viscous effects become important, and could strongly affect our conclusions. We do not pursue this further here and defer discussion of this viscous regime to a future publication. However, our results thus shed doubt on whether there is any region of parameter space in which the anisotropically-scaled equations (see §2.1 in the large Pr limit and §2.2 in the low Pr limit) apply. Indeed, by construction these equations are valid only when small-scale fluctuations are suppressed, but we see that this requires $Re_b \leqslant O(\alpha)$, in which case viscosity should play a dominant role in the mean equations and would impart a vertical lengthscale to the mean flow that is necessarily $O(Re^{-1/2})$ (c.f. Godoy-Diana *et al.* 2004; Cope *et al.* 2020).

4.2. *Regimes of stratified stellar turbulence*

Our findings partition parameter space into various regimes of stratified turbulence, which are illustrated in Figure 1 for a $Pr = 1$ fluid (top) and a $Pr = 10^{-6}$ fluid (bottom). The latter is typical of some stellar interiors (see Garaud 2021). In both panels, the horizontal axis shows the inverse Froude number Fr^{-1}, so that stratification increases to the right. The vertical axis shows the outer scale Péclet number Pe, so that diffusive effects decrease upward. In both panels, the grey region shows where α is $O(1)$, so the large-scale flow is isotropic; this regime is not the focus of this paper. For stronger stratification, the large-scale flow becomes anisotropic, and the possible regimes of stratified turbulence one may encounter depend on Pr.

For $Pr = O(1)$ (top figure) the partitioning of parameter space for $Fr^{-1} \gg 1$ is very simple. When $Pe_b, Re_b \geqslant O(1)$ (green region), viscosity and diffusion play a secondary role in both mean and fluctuation dynamics. This is the Chini *et al.* (2022) regime. By contrast, if $Pe_b, Re_b \ll O(1)$ (white region) then both begin to influence the flow dynamics and cannot be ignored. The transition takes place when $Re, Pe = O(Fr^{-2})$.

At low Pr, diffusion becomes important long before viscosity does, so the $Pe_b = O(1)$

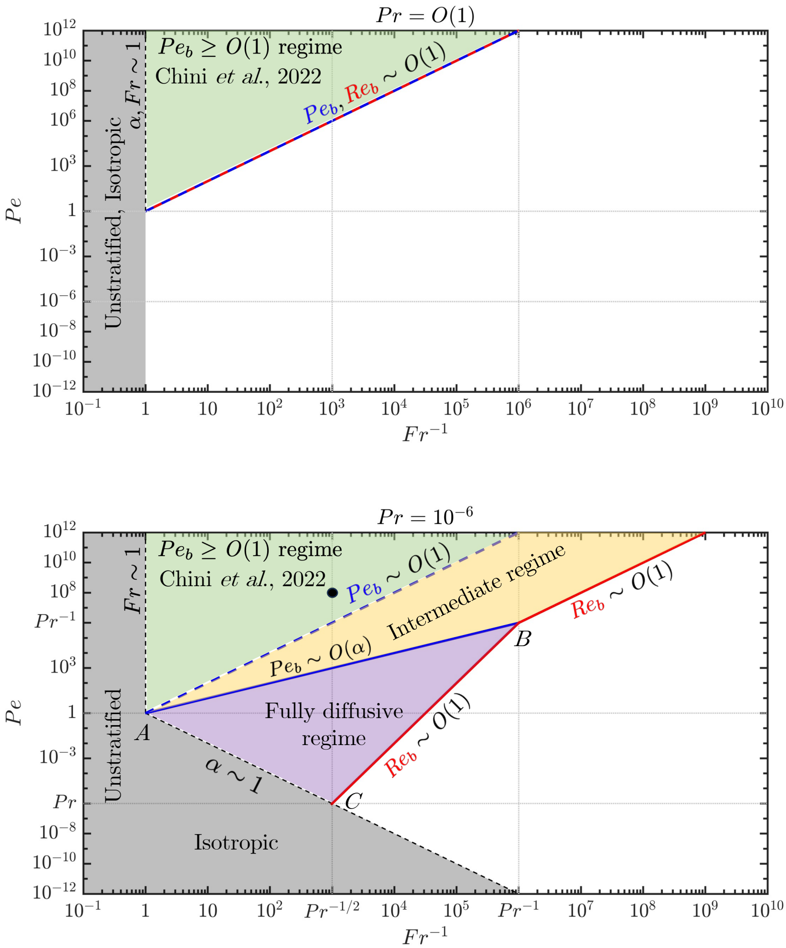

FIGURE 1. Regime diagram for a fluid with $Pr = 1$ (top) and a fluid with $Pr = 10^{-6}$ (bottom). The Péclet number is on the vertical axis the and inverse Froude number is on the horizontal axis (such that stratification increases to the right). Regions of unstratified, isotropic turbulence are marked in grey. Regions in white are viscously controlled, and will be discussed in future work. In both panels, the blue dashed line marks the transition $Pe_b = O(1)$ where the mean flow becomes diffusive, and the red solid lines mark the viscous transition where $Re_b = O(1)$. With $Pr \ll 1$ (bottom panel), it is possible to have $Pe_b \ll 1 \ll Re_b$, i.e. regimes of thermally diffusive stratified turbulence, which are not possible when $Pr = O(1)$. In that case, the solid blue line marks the transition where $Pe_b = O(\alpha)$ where the small-scale fluctuations become diffusive. We see that a region of parameter space opens up between $Pe_b = O(1)$ and $Re_b = O(1)$ where the two new regimes identified in this work exist: the intermediate regime, marked in yellow, and the fully diffusive regime marked in purple, bounded by the three corners of the triangle labelled A, B, C (see main text). The solar tachocline is marked in a black circle, using typical parameters given by Garaud (2020) ($Pe = 10^8$, $Fr^{-1} = 10^3$). For consistency with other grey lines, can you add a horizontal grey line at Pe = Pr? Also remove some of the white at bottom of figure – just need to crop it with e.g. Preview before uploading it to Overleaf

transition is distinct from the $Re_b = O(1)$ transition. This opens up parameter space to the two new regimes discussed in this work: the intermediate regime (yellow region, whose dynamics are described in §3.3.1) and the fully-diffusive regime (purple region, whose dynamics are described in §3.3.2). We now clearly see that the fully-diffusive regime is confined to a triangle in log-log parameter space. It is delimited from above by the intermediate regime (yellow region), from below by the isotropic regime (grey region), and from the right by the viscous regime (white region). More specifically, it is bounded by the points A ($Fr^{-1} = 1, Pe = 1$), B ($Fr^{-1} = Pr^{-1}, Pe = Pr^{-1}$) and C ($Fr^{-1} = Pr^{-1/2}, Pe = Pr$) and thus becomes increasingly wide as Pr decreases, but shrinks towards the point A as $Pr \to 1$.

A major implication of our results is that, depending on the choice of Pe, different regimes are encountered as stratification increases. We now discuss horizontal transects through Figure 1, for different values of Pe.

We first consider the case $Pr < Pe < 1$ which is the regime discussed in Cope *et al.* (2020). As Fr^{-1} increases, our model predicts that the turbulence ought to be isotropic until $Fr^{-1} = Pe^{-1/2}$ (this is because diffusion partially relaxes the effects of stratification when $Pe \ll 1$). As Fr^{-1} continues to increase, the turbulence enters the fully diffusive (anisotropic) regime, and remains in that regime until $Fr^{-1} = (Pe/Pr^3)^{1/4}$ at which point viscosity begins to affect the mean flow. This series of regime transitions is qualitatively consistent with what is observed in the low Prandtl number DNS of Cope *et al.* (2020). (We have converted their notation for this discussion.).

At the other extreme, let us consider a transect for $Pe > Pr^{-1}$, which is the case considered by Garaud (2020), who mainly looked at simulations where $Pe = 60$ and $Pr = 0.1$. It is a situation relevant for strongly sheared layers of stellar interiors, such as the solar tachocline. For moderate stratification, namely $1 \leqslant Fr^{-1} \leqslant Pe$, our analysis shows that the turbulence is expected to be both anisotropic and non-diffusive, and its properties should be captured by the model of Chini *et al.* (2022). As stratification increases past $Fr^{-1} = Pe$, the turbulence is predicted to enter the intermediate regime, where the mean flow is dominated by diffusion but the fluctuations are not. Beyond $Fr^{-1} = \sqrt{Pe/Pr}$, viscous effects should become important. Note how, at these large values of the Péclet number, the fully diffusive non-viscous regime discussed in §3.3.2 is not accessible. Instead, viscosity begins to influence the mean flow before diffusion influences the fluctuations.

This series of regime transitions is indeed qualitatively consistent with the simulations reported in Garaud (2020). (Once again, we have converted her notation for this discussion.) Specifically, she found that the turbulence is mostly isotropic for $Fr^{-1} < 1$, then becomes anisotropic with little effect of diffusion for intermediate values of Fr^{-1}. However, her empirically-derived scaling laws ($H^* \propto Fr^{2/3}L^*$, $W^* \propto Fr^{2/3}U^*$) do not match those predicted by the Chini *et al.* (2022) theory; future work will need to revisit the data to determine whether this discrepancy can be explained. For even larger values of Fr^{-1}, Garaud (2020) found that diffusion becomes important, and that the dynamics are governed by the LPN equations. However at this point the turbulence is also in an intermittent regime where viscosity partially suppresses the fluctuations. This is qualitatively consistent with predictions from Figure 1.

Finally, the case where $1 < Pe < Pr^{-1}$ is relevant for weaker shear layers in stellar interiors. As Fr^{-1} increases, our model predicts that the turbulence ought to be isotropic until $Fr^{-1} = 1$, at which point it enters the Chini *et al.* (2022) regime, where both mean and fluctuation equations are non-diffusive. As stratification continues to increase the vertical eddy scale decreases gradually until the mean flow becomes dominated by diffusion at $Fr^{-1} = \sqrt{Pe}$ and we enter the intermediate regime. The flow dynamics remain essentially unchanged in that regime until diffusion also begins to affect the fluctuations as well, at $Fr^{-1} = Pe$, at which point the turbulence becomes fully diffusive. Finally, viscous effects begin to be important when $Fr^{-1} = (Pe/Pr^3)^{1/4}$. To date, no DNS have been published probing this range of Pe. Verifying the existence of these successive transitions with DNS is one of our areas of active work.

4.3. *Mathematical considerations*

Having constructed a map of parameter space from our model predictions, we now discuss important consequences and caveats of the reduced model equations. As in Chini *et al.* (2022), we find that these form a closed set of equations describing the concurrent evolution of a highly anisotropic large-scale mean flow together with isotropic small-scale fluctuations. Crucially, the fluctuation equations derived in all regimes identified are linear, but feed back nonlinearly on the mean flow evolution. The reduced models derived thus all have a quasilinear form, which self-consistently emerges from the asymptotic expansion rather than being assumed *a priori*. The quasilinearity of the slow-fast equations therefore appears to be an inherent property of stratified turbulence regardless of the Prandtl number. Our findings can thus be used as a theoretical basis not only for using the quasilinear approximation to create reduced models of turbulence, but also to know precisely which terms to keep in each region of parameter space (see, e.g, Marston & Tobias 2023).

Put some sentences discussing need for scale separation in founding assumption, and whether it's true or not?

Nonlinear saturation in this type of quasilinear system requires it to reach a state of marginal stability for the fluctuations. It is easy to verify that this is indeed the case in each regime. In the $Pe_b \geqslant O(1)$ and intermediate regime, the fluctuation equations do not feel diffusion at leading order, and therefore describe the growth (or decay) of perturbations due to a standard vertical shear instability. The vertical shear of the mean flow can be estimated to be roughly $S^* = O(U^*/H^*)$ since $|\bar{\boldsymbol{u}}| = O(1)$. Its stability depends on the Richardson number, which is

$$J = \frac{N^2}{S^{*2}} = O\left(\frac{N^2 H^{*2}}{U^{*2}}\right) = O\left(\frac{\alpha^2}{Fr^2}\right) = O(1), \tag{4.4}$$

in these regimes, and therefore satisfies the well-known marginal stability condition of Richardson (1920). Note that Garaud *et al.* (2023) recently verified that J is indeed $O(1)$ in DNS of stratified turbulence at $Pe_b = O(1)$.

In the $Pe_b \ll \alpha$ regime, by contrast, the fluctuation equations are inherently diffusive, and one therefore expects the vertical shear instability to be of the diffusive kind (Zahn 1974; Jones 1977; Lignières *et al.* 1999). It has been shown, at least for sinusoidal shear flows (Garaud *et al.* 2015*a*), that the condition for marginal linear stability is $JPe_S = O(1)$ where $Pe_S = U^* H^*/\kappa$ is the Péclet number based on the vertical shear profile. We can easily check that the scalings found in Section 3.3.2 satisfy this criterion. Indeed,

$$JPe_S = O\left(\frac{N^2 H^{*2}}{U^{*2}} \frac{U^* H^*}{\kappa}\right) = O\left(\alpha^3 \frac{Pe}{Fr^2}\right) = O(1), \tag{4.5}$$

as required. Adding this evidence to the scaling laws derived from DNS data of Cope *et al.* (2020) confirms that (3.22) is indeed the correct expression for α in stratified turbulence at very low Pe_b.

A somewhat less intuitive result of this analysis is the requirement that $\partial \bar{p}_{00}/\partial \zeta = 0$ while $\bar{p}_{00} = O(1)$ in both intermediate and fully diffusive regimes. Physically-speaking, this condition can be understood by noting that in the $Pe_b \ll 1$ case, departures from the mean background stratification are formally very small, which explains why they do not affect the assumed *background* hydrostatic balance. Furthermore, recalling that ζ has been rescaled by the vertical lengthscale $H^* = \alpha L^*$ with $\alpha \ll 1$, we see that $\partial_\zeta \overline{p}_{00} = 0$ only applies on that scale, and does not preclude $\overline{p}_{00}$ from potentially varying on larger scales.

Greg can you work on this paragraph. Note that I'm not sure the expansions presented here work, so we all need to work out what is correct expansion (missing a p_{01} term I think). Higher order mean pressure terms, however, do depend on mean buoyancy via gradients in mean vertical velocity, for instance, in the fully diffusive case, $\partial_\zeta \overline{p}_{02} = (\partial_\zeta^2)^{-1}\overline{w}_{02} - \partial_\zeta \overline{w'_{01} w'_{01}}$ (need to write this in terms of $\bar{b}$ since this is what the text says) and in the intermediate regime, $\partial_\zeta \overline{p}_{10} = \overline{b}_{12}$. This higher-order dependence on the buoyancy offers a possible path for (weak) buoyancy effects to be incorporated into the mean dynamics of the reduced order model (4.3), which may be important on *larger vertical* scales. We do not pursue this path in the present study, but instead briefly outline it here for future work. In the horizontal momentum equation, $\overline{p}_{00}$ can be replaced by a composite pressure, $\overline{p}_c = \overline{p}_{00} + Pe_b\, \overline{p}_{10} + \alpha\, \overline{p}_{02}$. For consistency, the corresponding horizontal momentum equation accurate to $O(\alpha)$ should be derived in terms of a composite horizontal velocity, $\overline{\boldsymbol{u}}_{\perp c}$. Finally, we emphasize that buoyancy anomalies *do* affect the fluctuation dynamics.

5. Conclusions

In this study, we have leveraged numerical evidence of scale separation and flow anisotropy to conduct a formal, multiscale asymptotic analysis of the (Boussinesq) equations governing the dynamics of strongly stratified turbulence at low Prandtl number. A key outcome of our work is a new map of parameter space identifying different regimes of stratified turbulence, shown in Figure 1. Crucially, we find that new regions of parameter space open up at low Prandtl number in which diffusive turbulent flows exist, whereas this is not possible at $Pr = O(1)$. For each of these new regimes, scaling laws for the vertical velocity and vertical lengthscale of turbulent eddies naturally emerge from the analysis. These are summarized in §4.2 and recover previous findings by Chini *et al.* (2022) and Cope *et al.* (2020) in some distinguished limits. Finally, note that recent work by Garaud *et al.* (2023) has demonstrated numerically that the presence of a mean vertical shear (which was ignored in this work) has little impact on these scalings as long as its amplitude is smaller than the small-scale emergent vertical shear U^*/H^*. This finding can readily be proved more formally using the asymptotic tools developed here, and implies that the new map is robust (at least, ignoring other effects such as rotation and magnetic fields, see below).

These results have important implications for low Pr fluids, such as liquid metals (where $Pr \sim 0.01-0.1$), planetary interiors (where $Pr \sim 0.001-0.1$) and stellar interiors (where $Pr \sim 10^{-9} - 10^{-2}$). In particular, the scaling laws derived enable us to propose simple parameterizations for turbulent diffusion coefficients in each regime identified, by multiplying the characteristic vertical lengthscale and vertical velocity:

- In the $Pe_b \geqslant O(1)$ and the intermediate regimes,
$$D_{\text{turb}} \propto H^*W^* \propto Fr^{3/2} L^* U^* \propto U^{*\,5/2}/(L^{*\,1/2} N^{3/2}). \tag{5.1}$$
- In the fully diffusive regime,
$$D_{\text{turb}} \propto H^*W^* \propto (Fr^2/Pe)^{1/2} L^* U^* \propto U^{*\,3/2} \kappa^{1/2}/(L^{*\,1/2} N). \tag{5.2}$$

As such, our work challenges current understanding of stratified turbulence in stars.

Indeed, the most commonly used model for stratified turbulence in stellar evolution calculations is the model of Zahn (1992), which proposes a vertical turbulent diffusivity equivalent to (5.2). However, we have demonstrated that this expression is only valid in a relatively small region of the parameter space (see Fig. 1). In particular, Zahn's model assumes that the turbulence is always fully diffusive, but this is not the case in the intermediate and $Pe_b \geqslant O(1)$ regime, which are appropriate for more strongly sheared fluid layers such as the solar tachocline. Zahn's model also assumes that viscosity is negligible, which is not the case for sufficiently stratified flows.

Of course, future work will be needed to investigate the effects of rotation and magnetization, which are also important in stellar and planetary interiors. Both are likely to stabilize the horizontal turbulence to some extent, which will therefore affect the emergent vertical shear instability as well. Additionally, we need to systematically compare the model predictions with existing DNS (Brethouwer *et al.* 2007; Maffioli & Davidson 2016; Cope *et al.* 2020; Garaud 2020) as well as future DNS at more extreme values of the Reynolds, Prandtl, and Péclet numbers. In particular, known discrepancies between the model and data need to be explained (see §4.2). Furthermore, while we have so far compared scaling laws between model and data, we also need to verify whether the regime transitions are well-predicted by the theory. This step is crucial to gain enough confidence in the model to apply it at stellar and planetary parameter values. Nonetheless, this work has already demonstrated the power of formal asymptotic expansions for discovering and validating the existence of new regimes of stratified turbulence in stellar and planetary interiors.

MAYBE mention possible use of quasilinear approx for creating closure model for use in e.g. XX? not sure?

Other things to do:

- Bibliography needs to be tidied up – citations are in different formats because they have been pulled from different search engines. Need to figure out what JFM wants and fix them accordingly.

Acknowledgements

The authors gratefully acknowledge the Geophysical Fluid Dynamics Summer School (NSF 1829864). P.G. acknowledges funding from NSF AST-1814327. K.S. acknowledges funding from the James S. McDonnell Foundation.

Declaration of Interests

The authors report no conflict of interest.

REFERENCES

Billant, Paul & Chomaz, Jean-Marc 2001 Self-similarity of strongly stratified inviscid flows. *Physics of fluids* **13** (6), 1645–1651.

Brethouwer, Geert, Billant, Paul, Lindborg, Erik & Chomaz, J-M 2007 Scaling analysis and simulation of strongly stratified turbulent flows. *Journal of Fluid Mechanics* **585**, 343–368.

Chini, Gregory P, Michel, Guillaume, Julien, Keith, Rocha, Cesar B & Colm-cille, P Caulfield 2022 Exploiting self-organized criticality in strongly stratified turbulence. *Journal of Fluid Mechanics* **933**.

Cope, Laura, Garaud, Pascale & Caulfield, Colm-cille Patrick 2020 The dynamics of stratified horizontal shear flows at low Péclet number. *Journal of Fluid Mechanics* **903**.

Garaud, Pascale 2020 Horizontal shear instabilities at low Prandtl number. *The Astrophysical Journal* **901** (2).

Garaud, Pascale 2021 Journey to the center of stars: The realm of low prandtl number fluid dynamics. *Physical Review Fluids* **6** (3), 030501.

Garaud, Pascale, Gallet, Basile & Bischoff, Tobias 2015*a* The stability of stratified spatially periodic shear flows at low Péclet number. *Physics of Fluids* **27** (8), 084104, arXiv: 1507.07286.

Garaud, Pascale, Khan, Saniya & Brown, Justin M. 2023 The combined effects of vertical and horizontal shear instabilities. *arXiv e-prints* p. arXiv:2308.14442, arXiv: 2308.14442.

Garaud, P., Medrano, M., Brown, J. M., Mankovich, C. & Moore, K. 2015*b* Excitation of Gravity Waves by Fingering Convection, and the Formation of Compositional Staircases in Stellar Interiors. *ApJ* **808** (1), 89, arXiv: 1505.07759.

Godoy-Diana, Ramiro, Chomaz, Jean-Marc & Billant, Paul 2004 Vertical length scale selection for pancake vortices in strongly stratified viscous fluids. *Journal of Fluid Mechanics* **504**, 229–238.

Holford, Joanne M. & Linden, P. F. 1999 Turbulent mixing in a stratified fluid. *Dynamics of Atmospheres and Oceans* **30** (2), 173–198.

Jones, C. A. 1977 The Onset of Shear Instability in Stars. *Geophysical and Astrophysical Fluid Dynamics* **8**, 165–184.

Lignières, F. 1999 The small-Péclet-number approximation in stellar radiative zones. *A&A* **348**, 933–939, arXiv: astro-ph/9908182.

Lignières, François 2020 Turbulence in stably stratified radiative zone. In *Multi-Dimensional Processes In Stellar Physics*, pp. 111–140. EDP Sciences.

Lignières, F., Califano, F. & Mangeney, A. 1999 Shear layer instability in a highly diffusive stably stratified atmosphere. *Astron. Astrophys.* **349**, 1027–1036, arXiv: astro-ph/9908184.

Maffioli, Andrea & Davidson, Peter A 2016 Dynamics of stratified turbulence decaying from a high buoyancy reynolds number. *Journal of Fluid Mechanics* **786**, 210–233.

Marston, J. B. & Tobias, S. M. 2023 Recent Developments in Theories of Inhomogeneous and Anisotropic Turbulence. *Annual Review of Fluid Mechanics* **55**, 351–375, arXiv: 2205.05513.

Oglethorpe, R. L. F., Caulfield, C. P. & Woods, Andrew W. 2013 Spontaneous layering in stratified turbulent Taylor-Couette flow. *Journal of Fluid Mechanics* **721**, R3.

Richardson, L. F. 1920 The Supply of Energy from and to Atmospheric Eddies. *Royal Society of London Proceedings Series A* **97**, 354–373.

Skoutnev, Valentin A. 2023 Critical balance and scaling of strongly stratified turbulence at low Prandtl number. *Journal of Fluid Mechanics* **956**, A7, arXiv: 2205.01540.

Spiegel, Edward A & Veronis, G 1960 On the boussinesq approximation for a compressible fluid. *The Astrophysical Journal* **131**, 442.

Spiegel, E. A. & Zahn, J. P. 1970 Instabilities of Differential Rotation. *Comments on Astrophysics and Space Physics* **2**, 178.

Zahn, Jean-Paul 1974 Rotational instabilities and stellar evolution. In *Symposium-International Astronomical Union*, , vol. 59, pp. 185–195. Cambridge University Press.

Zahn, J-P 1992 Circulation and turbulence in rotating stars. *Astronomy and Astrophysics* **265**, 115–132.